Journal of Power Sources 228 (2013) 294–299

Contents lists available at SciVerse ScienceDirect

Journal of Power Sources

journal homepage: www.elsevier.com/locate/jpowsour

Cycling profile of innovative nanochitin-incorporated poly (ethylene oxide) based electrolytes for lithium batteries

N. Angulakhsmi [a], S. Thomas [b], Jijeesh R. Nair [c], R. Bongiovanni [c], C. Gerbaldi [c], A. Manuel Stephan [a,*]

[a] EPS Division, Central Electrochemical Research Institute (CSIR-CECRI), Karaikudi 630006, India
[b] Mahatma Gandhi University, Kottayam 686560, India
[c] Department of Applied Science and Technology (DISAT), Politecnico di Torino, Corso Duca degli Abruzzi 24, 10129 Torino, Italy

HIGHLIGHTS

- Nanocomposite polymer electrolytes have been identified as separators for safe batteries.
- Nanochitin has been incorporated in poly (ethylene oxide) matrix for the first time.
- A high discharge capacity of 150 mA h g^{-1} at C/5-rate has been achieved even at 70 °C.
- The overall performance of Li/NCPE/$LiFePO_4$ cell is better than the earlier reports.

GRAPHICAL ABSTRACT

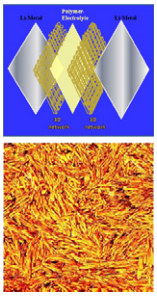

ARTICLE INFO

Article history:
Received 3 September 2012
Received in revised form
6 November 2012
Accepted 8 November 2012
Available online 24 November 2012

Keywords:
Nanocomposite polymer electrolytes
Chitin
Ionic conductivity
Compatibility
Discharge capacity

ABSTRACT

Nanochitin has been incorporated in a poly (ethylene oxide) (PEO)-$LiPF_6$ matrix for the first time. The incorporation of chitin whiskers significantly improves the ionic conductivity, thermal stability, mechanical integrity along with the interfacial properties. The prepared membrane is also tested in a $LiFePO_4$/C—Li cell and the galvanostatic cycling behaviour is analysed at 70 °C showing an improved specific capacity and outstanding cycling stability. The obtained results and the use of such environment friendly component would make these hybrid organic, nanochitin-based composite polymer electrolyte systems a strong contender in the field of flexible and green lithium-based power sources.

1. Introduction

The effect of global warming, fluctuation of oil prices, dwindling resources of fossil fuels and revolution in the portable electronic devices have forced researchers to find alternative energy storage systems. Lithium-ion batteries, supercapacitors and fuel cells are considered strongly as major contenders for power source applications. Rechargeable lithium-ion batteries are extensively used in consumer electronic products including laptop computers, cellular phones, cameras, camcorders and medical devices [1–4]. The state-of-the-art lithium ion batteries employ many variations in cell components and chemistries. Most of them use a graphitic carbon anode (negative electrode), a liquid electrolyte comprised of lithium salts dissolved in organic solvents, a microporous polymer separator and lithium intercalated transition-metal oxide cathode (positive electrode). The solid polymer electrolyte has several

* Corresponding author. Tel.: +91 4565 241 426; fax: +91 4565 227 779.
E-mail addresses: amstephan@cecri.res.in, arulmanuel@gmail.com (A.M. Stephan).

0378-7753/$ – see front matter © 2012 Elsevier B.V. All rights reserved.
http://dx.doi.org/10.1016/j.jpowsour.2012.11.007

advantages over its liquid counterpart such high energy density, no-leakage of electrolyte and flexible geometry [5]. The prerequisites of solid polymer electrolytes for lithium battery applications are (i) high ionic conductivity, (ii) good transference number,(iii) better interfacial property, (iv) good mechanical integrity and (v) appreciable thermal stability.

Poly (ethylene oxide) as a host has been most extensively studied for battery applications. PEO chains adopt a helical conformation with all the C–O bonds in trans and the C–C bonds in either gauche or gauche minus configuration [5]. In this geometry, cations can be located in each turn of the helix and are coordinated by three ether oxygens. However, the basic structure of the host is retained for all sizes of anions. PEO is a good polymer electrolyte but suffer from poor mechanical strength and limited thermal resistance: these properties are required for safety and performance reasons, in addition to high ionic conductivity and a wide electrochemical stability window.

The introduction of reinforcing particles has been first proposed by Weston and Steele [6] and in the recent years nanosized fillers have been preferred [7–10]. Alternatively, fibres, nanofibres and whiskers have been employed, preferably of natural origin e.g. cellulose microfibrils [10] and cellulose whiskers [11–13]. In the present study, chitin was employed as novel inert filler in solid polymer electrolytes. Chitin is a long complex polysaccharide made up of repeating units of the disaccharide acetyl glucosamine. Chitin, poly (β-(1-4)-*N*-acetyl-D-glucosamine), is the most abundant biopolymer after cellulose [11]. Chitin occurs as ordered crystalline microfibrils and is useful in applications that require reinforcement and strength. Chitin is available in two allomorphs, namely, α and β forms, which can be differentiated by infrared, solid-state nuclear magnetic resonance (NMR), and X-ray diffraction (XRD) spectroscopy [12]. Chitin has low toxicity, biodegradability and antibacterial properties. It also possesses gel-forming properties and finds many applications. Chitin is used as an additive to thicken and stabilize foods and pharmaceuticals, acts as a binder in dyes, fabrics and adhesives. Industrial separation membranes and ionic exchange resins can be made from chitin, finally it has been used as a biosensor [11–13]. To the best of our knowledge; chitin has never before been investigated as filler in nanocomposite polymer electrolytes for battery applications.

Recent studies indicate that membranes prepared by conventional solvent casting method lead to poor interfacial properties at the lithium/polymer electrolyte interface. Impurities, mostly the traces of solvent, are trapped in the high surface area, nanosized inert fillers in solvent-cast electrolytes, even after prolonged drying [14]. Hence, in the present study the hot press technique was employed for the preparation of nanocomposite polymer electrolytes.

2. Experimental procedure

In order to remove the proteins, the chitin precursor was boiled and stirred with 5% aqueous solution of KOH. It was then washed with distilled water and dried and this procedure was repeated three times. The bleaching solution was prepared by dissolving 17 g of NaCl in 1 l of water with 0.3 M sodium acetate as buffer and the sample was bleached at 80 °C for 6 h. The bleaching solution was changed every 2 h. For further removal of residual proteins the chitin suspension was bleached in 5% KOH for 72 h, centrifuged at 3000 rpm for 20 min and hydrolysed with 3 N HCl under continuous stirring for 1.5 h. The suspension was dialysed in a dialyses bag for 24 h until its pH reached the value of 6 and further the pH of the suspension was adjusted to 3.5 with HCl. The dispersed viscous suspensions were treated ultrasonically and filtered to remove residual aggregates. The resulting nanochitin was refrigerated with sodium – azoture as a protectant against microorganisms. The prepared nanochitin particle size was found to be between 400 and 500 nm of length and diameter of 1 nm and its atomic force microscopy (AFM) picture is displayed in Fig. 1.

PEO (M_w = 200,000, Sigma–Aldrich) and $LiPF_6$ (Sigma–Aldrich) were dried under vacuum for 2 days at 50 and 60 °C, respectively. Polymeric membranes were prepared as follows. The composition of PEO, chitin and $LiPF_6$ are shown in Table 1 and are denoted as samples S1–S5. In order to get a homogeneous polymeric membrane, appropriate amounts of PEO, $LiPF_6$ and chitin were dissolved in acetonitrile, stirred for 6 h and casting the solute in Teflon sheet. The resulting mass was hot-pressed into films as described elsewhere [14].

The films had an average thickness of 30–50 μm. This procedure yielded homogeneous and mechanically strong membranes, which were dried under vacuum at 50 °C for 24 h for further characterization. The ionic conductivity of the membranes sandwiched between two stainless steel blocking electrodes (area 1 cm^2 diameter) was measured using an electrochemical impedance analyser (IM6-Bio Analytical Systems) in the 50 mHz to 100 kHz frequency range at various temperatures (0, 15, 30, 40, 50, 60 and 70 °C). The bulk resistance of the polymer electrolyte was found from the impedance spectrum. Thus, the ionic conductivity was calculated based on the equation [15]:

$$\sigma = (l/A) \times (1/R_b)\left(\mathrm{S\ cm^{-1}}\right)$$

where σ is the ionic conductivity, R_b the bulk resistance; l and A are the thickness of the membrane and area of the specimen, respectively. Symmetric non-blocking cells of the type Li/NCPE/Li were assembled for compatibility studies and were investigated by studying the time dependence of the impedance of the systems under open circuit condition at 70 °C.

The mechanical strength of the nanocomposite polymer electrolytes (NCPE)'s was determined using a tensile machine (Tinius Olsen) with a constant cross-head speed of 10 mm min^{-1}. The sample was prepared exactly by following the instructions given

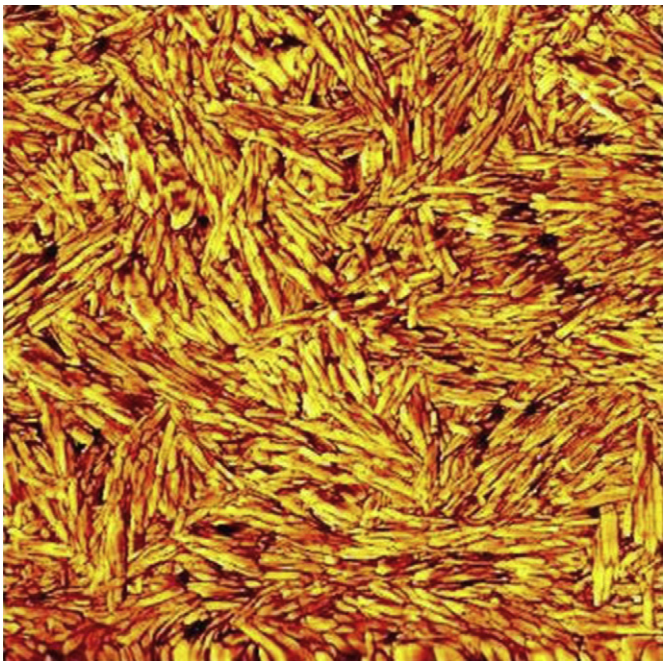

Fig. 1. AFM image of chitin.

Table 1
Composition of PEO, chitin and lithium salt.

Sample	PEO (wt.%)	Chitin (wt.%)	$LiFF_6$ (wt.%)
S1	95	0	5
S2	90	5	5
S3	85	10	5
S4	77	17	5
S5	75	20	5

by ASTM Standard D638. Temperature modulated Differential scanning calorimetry (TM-DSC) (Mettler Toledo, Switzerland) measurements were performed at a rate of 10 °C min^{-1} between −100 and +100 °C while TG-DTA (TA Instruments, USA) in the temperature range between 20 and 400 °C. Morphological study of the films was made by a scanning electron microscopy (SEM; Hitachi S-4700 FESEM) under a vacuum condition (10^{-1} Pa) after sputtering gold on one side of the films. X-ray diffraction (XRD) measurements were conducted on a Bruker D8 X-ray diffractometer with Cu-Kα radiation ($\lambda = 1.54178$ Å) at 50 kV and 250 mA with a scanning rate of 2° min^{-1}. The $LiFePO_4$/C cathode material was synthesised in the form of nanostructured powder through a mild hydrothermal procedure developed at Politecnico di Torino and described in details by Meligrana et al. [16]. The composite cathode was prepared in the form of a film (average thickness of about 70 μm) by blending 10 wt.% of poly (vinylidene fluoride) as the binder (SolvaySolef 6020) with 20 wt.% of acetylene black (Shawinigan Black AB50, Chevron Corp., USA) as the electronic conductivity enhancer and 70 wt.% of $LiFePO_4$/C active material, thoroughly mixed in 1-methyl-2-pyrrolidone (NMP, Aldrich). The paste was coated by a doctor-blade process onto an aluminium foil current collector. After the complete evaporation of the NMP solvent by mild heating and progressive vacuum treatment for 24 h, electrode disks of 2.54 cm^2 were punched out and dried under high vacuum at 130 °C for 5 h. The lithium polymer cell was fabricated by laminating the three components in sequence, i.e. a lithium metal anode foil, a layer of the NCPE membrane and the $LiFePO_4$/C composite cathode film. The assembly was housed into a hermetically sealed test cell (model ECC-Std, http://el-cell.com/products/testcells/ecc-std, purchased from EL-Cell, Germany). All preparations were performed in an argon- filled glove box (MBraun Labstar, Germany) having a humidity content below 1 ppm.

The characteristics and performances of the all-solid lithium polymer cell were investigated at 70 °C in terms of charge/discharge galvanostatic cycling by an Arbin Instrument Testing System model BT-2000, setting the cut off voltages to 2.50–4.00 V versus Li/Li^+. The charge–discharge cycles were set at the same rate at C/5 (34 mA g^{-1}) current rate.

3. Results and discussions

The typical SEM images of PEO + $LiPF_6$ and PEO + chitin + $LiPF_6$ (NCPE sample S3 made of 85% PEO + 10% chitin + 5% $LiPF_6$) membranes obtained by hot pressing technique and are displayed in Fig. 2. According to Chu et al. [17] that the morphology of the electrolyte surface can be modified/tailored by the incorporation of both ionic salts and fillers. The SEM images of PEO + $LiClO_4$ membranes given in Fig. 2(a) shows a smooth surface (with 5 wt.% $LiClO_4$). SEM image of nanochitin-incorporated membrane (Fig. 2(b)) also shows a similar surface, which suggests sufficiently good miscibility of nanochitin with the polymer and lithium salt. The smooth morphology is attributed to cross-linking of polymer with both lithium ions and nanochitin. However, at high contents of nanochitin (about 17 wt.%), the membrane is seen to have a rough surface with an inhomogeneous morphology with islands of aggregated particles (Figure not given).

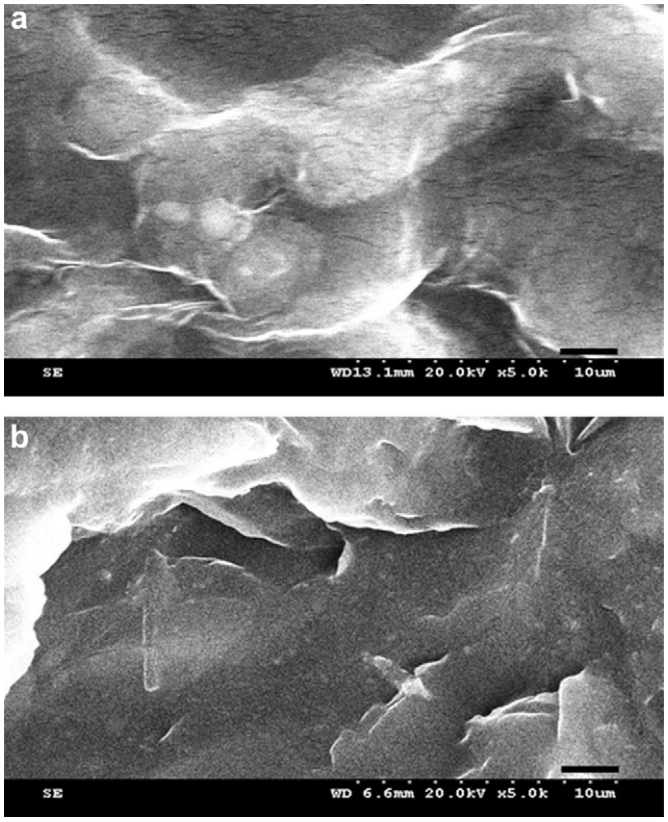

Fig. 2. SEM images of polymer electrolytes composed of (a) PEO + $LiPF_6$ and (b) PEO + $LiPF_6$ + chitin.

Fig. 3 (a–d) displays the XRD pattern of PEO (a), chitin (b), polymer electrolyte (c), comprising PEO + $LiPF_6$ and nanocomposite polymer electrolyte (NCPE) (d) composed of PEO + chitin + $LiPF_6$ respectively. Upon incorporation of $LiPF_6$ in the PEO host, (Fig. 3(c)), peaks corresponding to $LiPF_6$ are not observed, indicating that the $LiPF_6$ is completely dissolved. The crystallinity in the polymer originates from the ordering of poly ether side chains [17,18]. Apparently from Fig. 3(a and d) the

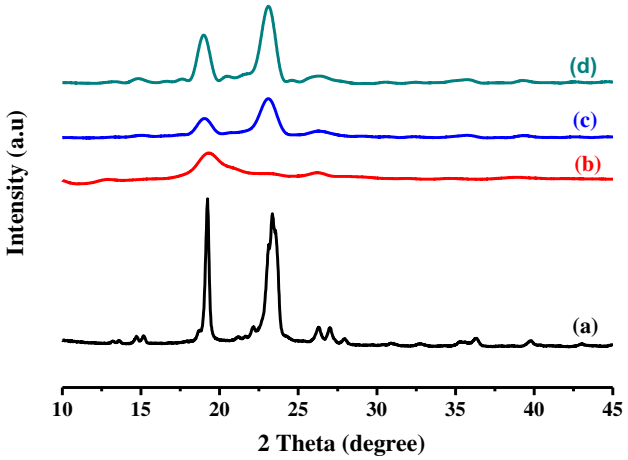

Fig. 3. XRD pattern of (a) pure PEO (b) nanochitin (c) PEO + $LiPF_6$ and (d) PEO + chitin + $LiPF_6$.

crystalline nature of PEO has been considerably reduced with the addition of chitin into the polymer matrix. Upon the addition of nanochitin and lithium salt in the polymer matrix, the crystallinity of the polymer has been significantly reduced and this reduction is attributed to the re-organisation of polymeric chains by the small inert particles present in nanocomposite electrolytes. This reorganization facilitates higher ionic conduction.

The TG-DTA traces of PEO, samples S1 (95% PEO + 5% $LiPF_6$) and S3 (85% PEO + 10% chitin + 5% $LiPF_6$) are shown in Fig. 4(a and b). Generally the heating process brings a lot of changes in the nanocomposite electrolytes, finally leaving behind inert residues. A weight loss of around 3% has been observed around 50 °C and is attributed to the removal of moisture absorbed at the time of loading the sample. An irreversible degradation of PEO starts at around 190 °C [19]. The degradation of PEO + $LiPF_6$ starts around at 210 °C whereas that of PEO + $LiPF_6$ + chitin starts at 290 °C. The enhanced thermal stability of chitin-added nanocomposite electrolytes may be attributed to the intercalation/exfoliation of the polymer matrix with inert particles, which resulted in a strong barrier effect preventing from the thermal degradation to a certain extent and this observation is an indication of the fact that PEO + $LiPF_6$ + chitin is stable up to a temperature of 275 °C in nitrogen atmosphere [19].

Fig. 5 depicts the DSC traces for the samples S1 and S3. In the present study, DSC measurements were performed in the temperature range of −100 °C to 100 °C. The sample S1 (without chitin) showed a glass transition temperature at −72 °C, and the melting point at 55 °C whereas nanochitin-incorporated sample S3 showed

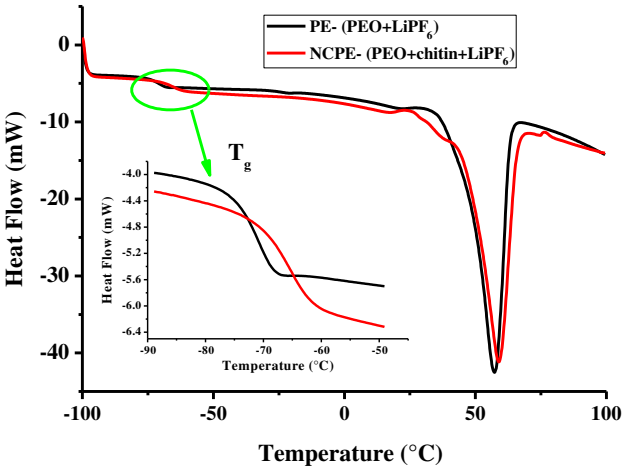

Fig. 5. Differential scanning calorimetry (a) PE (black curve) and (b) NCPE (red curve). Inset: Glass transition temperature of without (PE) and with filler (NCPE). (For interpretation of the references to colour in this figure legend, the reader is referred to the web version of this article.)

a heat inflection at higher temperature with an increase of about 9 °C (i.e. −63 °C) and a slightly higher melting point, T_m. The addition of chitin fillers has a small effect on the T_g which may be associated with two counteracting phenomena, i.e. PEO amorphization by lithium salt which weakly decrease the T_g value and chitin/PEO interactions which may increase the T_g value. The increase in T_g value by the addition of chitin could be attributed to the interaction between the acidic hydrogen of amide group of the chitin chain and the oxygen of the amorphous ethylene oxide (−EO−) repeating units which creates the effect similar to hydrogen bonding. This in turn reduces the segmental mobility of the amorphous PEO chains (a kind of physical cross-linking of amorphous −EO− chains) thus resulting in an increase in the T_g value. As the degree of crystallinity is not modified upon addition of chitin, the invariance of T_g may be related to the predominant effect of chitin/PEO interactions compared to lithium ion/PEO interactions [20].

In order to quantify the mechanical strength, the stress−strain property has been measured and the results are shown in Fig. 6. The stress−strain behaviour gives fundamental information about the load vs. deformation characteristics of polymer composites. In

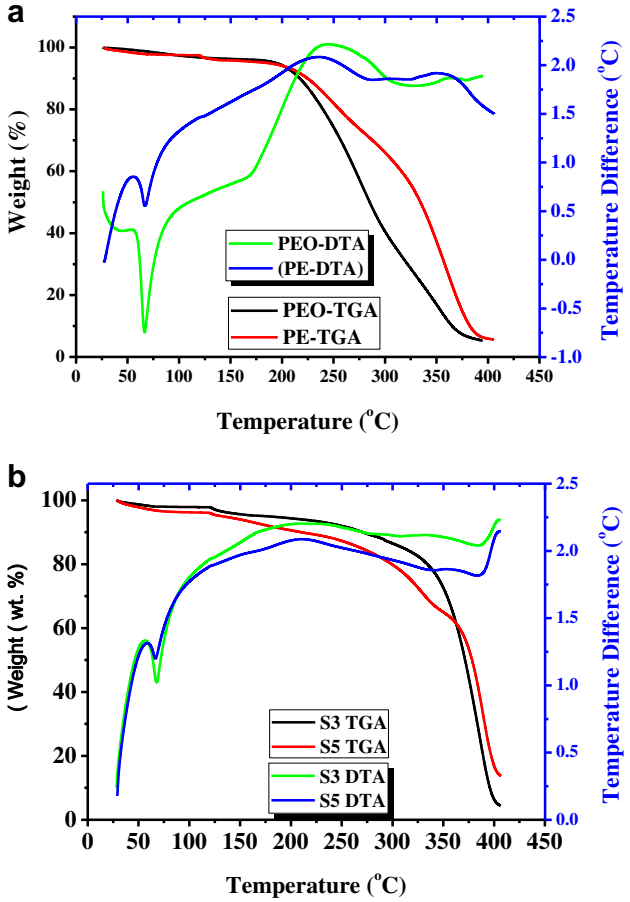

Fig. 4. (a) TG-DTA traces of neat PEO and PE (PEO + $LiPF_6$). (b) TG-DTA traces of NCPE with two different concentrations of chitin (sample S3 and S5).

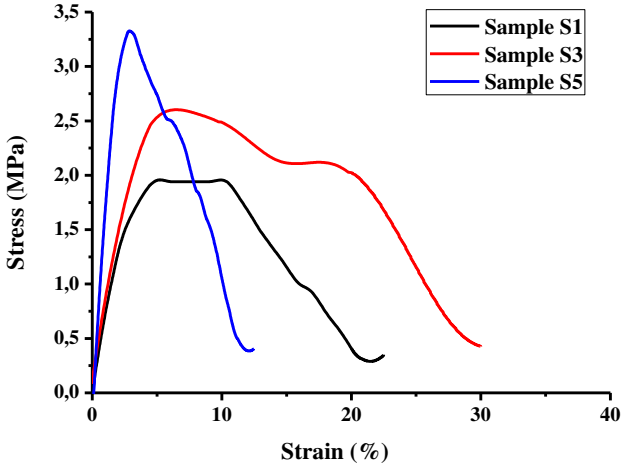

Fig. 6. Stress vs. strain curves for various concentrations of filler (S1) 0%, (S3) 10% and (S5) 20% of chitin.

Fig. 6 two distinct regions are evidenced: the initial linear region reflects the elastic characteristics and the non-linear region shows the plastic deformation. The tensile strength of the sample S3 (85% PEO + 10% chitin + 5% $LiPF_6$) has been increased from 1.9 MPa to 2.6 MPa with an addition of 10 wt.% of chitin in to the polymer matrix. Further addition of nanochitin also increases its modulus value from 2.6 MPa to 3.3 MPa. But the overall elongation at break was reduced from 22% (S1) to 12% (S5) [21]. Indeed an optimum elongation at break was observed for sample S3. At higher concentrations of nanochitin the tensile strength decreases as a result of aggregation of nanochitin particles which in turn non homogeneously dissipate the applied stress through the membrane.

The variation of ionic conductivity as a function of inverse of temperature is depicted in Fig. 7 for various concentrations of nanochitin. It can be seen from Fig. 7 that the ionic conductivity increases with the increase in temperature. All the curves show a slow and continuous change in the slope up to around 60 °C, beyond which there is a remarkable change in slope, reflecting the well-known transition from the crystalline to the amorphous phase of PEO. This transition contributes to an increase in ionic conductivity which clearly illustrates that incorporation of nanochitin enhances the ionic conductivity up to one order magnitude. These results are in accordance with those reported on PEO-based polymer electrolytes with SiO_2–lithium imide anion systems [22–24].

According to Wieckzorek et al. [25] the Lewis base reactions between the filler surface and the PEO segments may induce structural modifications in the polymer matrix. The Lewis acid character of the added ceramics (γ-Al_2O_3) would compete with the Lewis acid character of the lithium cations for the formation of complexes with the PEO chains. In the present study, chitin would act as cross-linking centres for the PEO segments, which lowers the polymer chain reorganization tendency, thus promoting an overall stiffness to the structure. However, the resulting structure provides Li^+-conducting pathways at the filler surface and enhances ionic transport [26].

The solid polymer electrolyte–lithium interface plays a vital role in the electrochemical behaviour of the lithium-polymer cells [27]. Fig. 8(a) shows the variation of the interfacial resistance as a function of time for the symmetric cells Li/NCPE/Li at 70 °C. The interfacial properties of lithium metal anode in contact with the electrolyte are critical in practical applications. The interfacial resistance values increase and decrease in an irregular manner. This may be attributed by assuming that the morphology of the passivation films changes with time and finally acquire a non-compact, possibly porous structure [28]. However, the values of the interfacial resistance of chitin-added samples are substantially lower than that of the filler-free samples. Furthermore, the interfacial resistance remained stable over long periods of storage (240 h). The considerable decrease in the interfacial resistance of chitin-added membranes may be attributed to the formation of a chitin–chitin three-dimensional network [29–31]. (Fig. 8(b)) which may minimize the area of the lithium metal anode exposed to polymer and thus reduce the passivation process.

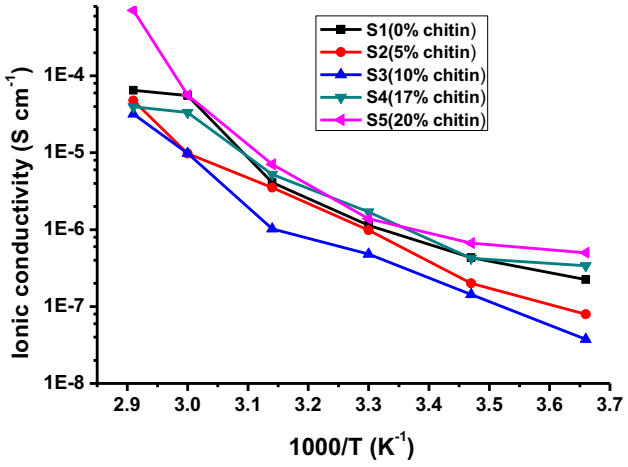

Fig. 7. Ionic conductivity as a function of $1/T$ as various concentrations of filler chitin.

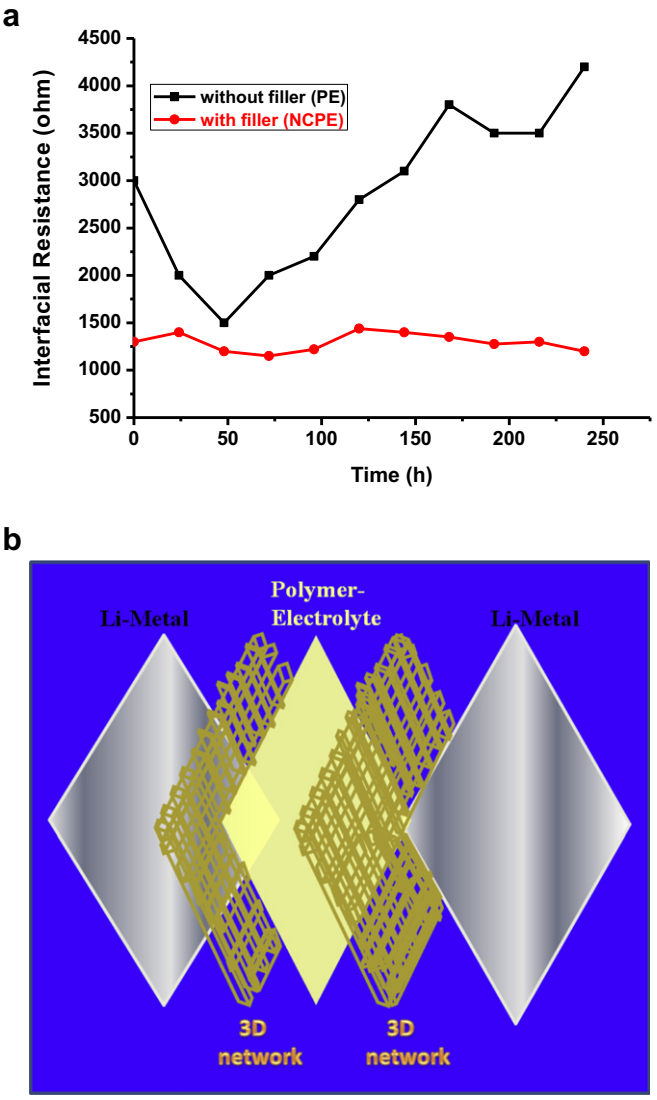

Fig. 8. a) Interfacial resistance as a function of time of polymeric membranes. (b) Schematic representation of chitin – three dimensional network with lithium metal anode.

High ionic conductivity and stable interfacial properties are some of the desirable properties for battery applications; hence, we have selected the NCPE (S3) membrane for further electrochemical characterization. A laboratory scale truly solid lithium cell was assembled, by combining a lithium metal anode with a $LiFePO_4$/C cathode and using the NCPE (PEO + chitin + $LiPF_6$) as the all-solid electrolyte, and tested in order to evaluate the capability of the electrolyte to perform in a real battery configuration. Its electrochemical behaviour was investigated by means of galvanostatic charge/discharge cycling performed at 70 °C. Lithium iron phosphate ($LiFePO_4$), belonging to the olivine type compounds, was

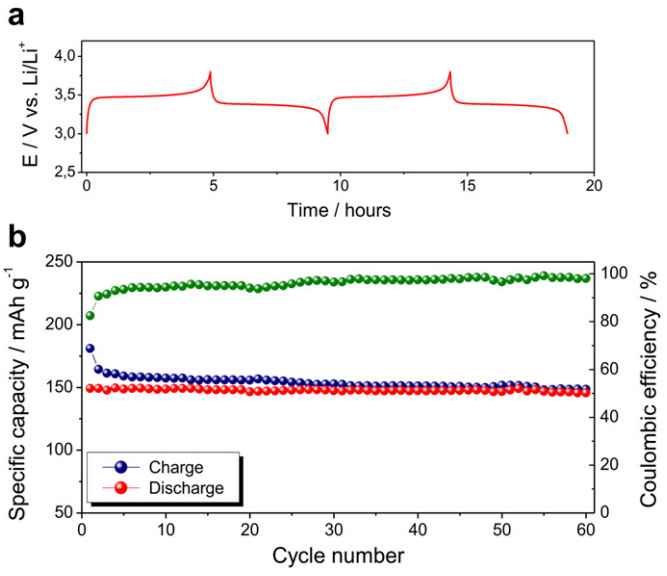

Fig. 9. Cycling profile of Li/NCPE(PEO + chitin + $LiPF_6$)/$LiFePO_4$ at 70 °C of (a) potential vs. Li^+/Li as a function of time (h) and (b) specific capacity (mA h^{-1} g) vs. cycle number.

selected as cathode material because it exhibits a high theoretical capacity and a flat charge/discharge profile. Additionally, the cost effectiveness, environmental and safety returns (high abuse tolerance), thermal stability at fully charged state, and reasonably good cyclability have made $LiFePO_4$ as one of the most attractive cathode materials for rechargeable Li-based batteries.

The typical charge and discharge (voltage vs. time) profiles obtained at 70 °C between 3.0 and 3.6 V vs. Li/Li^+ at C/5 − rate is shown in Fig. 9(a). The polymer cell showed voltage plateau at 3.45 V. It can be seen from the figure that the charge and discharge plateaus are highly reproducible and well defined. Fig. 9(b) shows the resulting plot of specific capacity vs. cycle number at C/5 rate (about 0.15 mA with respect to a $LiFePO_4$ active mass of about 4 mg). In the initial charge process, the specific capacity approaches almost full capacity, which rapidly reduces to about 155 mA h g^{-1} and, then, remains almost stable after the 10th cycle. The cell delivers an initial specific discharge capacity of about 150 mA h g^{-1} with a reasonable capacity retention. Even after 60 cycles the cell delivers a specific capacity of 146 mA h g^{-1}. A similar observation has been reported by Appetecchi et al. [32] where the authors reported the cycling behaviour of PEO/$LiCF_3SO_3$/SiO_2-based NCPE at 90 °C. However, the above system exhibited a fade in capacity of about 0.3 mA h g^{-1} per cycle, while our cell exhibits better cycling performance demonstrating a capacity fading of less than 0.1 mA h g^{-1} per cycle which accounts for a negligible degradation of all the components of the polymer cell. Thus, the cell operates with the expected voltage profile delivering a high fraction of the theoretical capacity. The coulombic efficiency is also found to be higher than 98%. The performance of this cell indicates a good interfacial contact between electrodes and polymer electrolyte, charge transport between electrodes and electrolyte of the cell.

4. Conclusions

Nanochitin-incorporated poly (ethylene oxide) based electrolytes were prepared for the first time and their both physical and electrochemical properties have been analysed. The lithium cell comprising Li/NCPE/$LiFePO_4$ has exhibited high discharge capacity than those reported earlier at a low temperature. The results here discussed, although preliminary, demonstrate the feasibility of the nanochitin incorporated PEO-based membrane as an innovative electrolyte which guarantees for an all-solid-state lithium-polymer battery at elevated temperature applications.

References

[1] J.M. Tarascon, M. Armand, Nature 414 (2001) 359–367.
[2] M. Armand, J.M. Tarascon, Nature 451 (2008) 652–657.
[3] D. Linden, T. Reddy, Handbook of Batteries, third ed., McGraw Hill, New York, 2001, p. 382.
[4] V. Subramaniyan, C. Luo, A. Manuel Stephan, K.S. Nahm, Sabu Thomas, B. Wei, J. Phys. Chem. C 111 (2007) 7527–7531.
[5] Y.G. Andrew, P.G. Bruce, Electrochim. Acta 45 (2000) 1417–1423.
[6] J. Weston, B.C.H. Steele, Solid State Ionics 7 (1982) 75–79.
[7] F. Croce, R. Curini, A. Martinelli, L. Perci, F. Ronci, B. Scrosati, J. Phys. Chem. B 103 (1999) 10632–10638.
[8] B. Scrosati, F. Croce, S. Panero, J. Power Sources 100 (2001) 93–97.
[9] A. Manuel Stephan, T. Prem Kumar, N. Angulakshmi, R. Bongiovanni, J.R. Nair, J. Appl. Polym. Sci. 124 (2012) 3245–3254.
[10] A. Chiappone, J.R. Nair, C. Gerbaldi, L. Jabbour, R. Bongiovanni, E. Zeno, N. Penazzi, D. Beneventi, J. Power Sources 196 (2011) 10280–10288.
[11] M. Rinaudo, Prog. Polym. Sci. 31 (2006) 603–632.
[12] K.M. Rudall, W. Kenchington, Bio. Rev. 40 (1973) 597–612.
[13] B. Krajewska, Enz. Microbio. Tech. 35 (2004) 126–139.
[14] J.H. Shin, F. Alessandrini, S. Passerini, J. Electrochem. Soc. 152 (2005) A283–A288.
[15] C.A. Vincent, B. Scrosati, Modern Batteries. An Introduction to Electrochemical Power Sources, Second ed., Arnold, London, 1993.
[16] G. Meligrana, C. Gerbaldi, A. Tuel, S. Bodoardo, N. Penazzi, J. Power Sources 160 (2006) 516–522.
[17] P.P. Chu, M.J. Reddy, H.M. Kao, Solid State Ionics 156 (2003) 141–153.
[18] P.S. Anantha, K. Hariharan, Solid State Ionics 176 (2005) 155–162.
[19] T. Shodai, B.B. Owens, M. Ostsuka, J. Yamaki, J. Electrochem. Soc. 141 (1994) 2978–2981.
[20] A. Manuel Stephan, T.P. Kumar, M.A.K. Nathan, N. Angulakshmi, J. Phys. Chem. B 113 (2009) 1963–1971.
[21] S.P. Thomas, S. Thomas, S. Bandyopadhyay, J. Phys. Chem. C 113 (2009) 97–104.
[22] L.Z. Fan, J. Maier, Electrochem. Comm. 8 (2006) 1753–1756.
[23] C.D. Robitaille, D. Fauteux, J. Electrochem. Soc. 133 (1986) 315–325.
[24] C. Capiglia, P. Mustarelli, E. Quartarone, C. Tomasi, A. Magistris, Solid State Ionics 118 (1999) 73–79.
[25] W. Wieczorek, Z. Florjancyk, J.R. Steven, Electrochim. Acta 40 (1995) 2251–2258.
[26] J. Przluski, M. Siekierski, W. Wieczorek, Electrochim. Acta 40 (1995) 2101–2108.
[27] Q. Li, N. Imanashi, A. Hirano, Y. Takeda, O. Yamamoto, Solid State Ionics 159 (2003) 97–109.
[28] G.B. Appetecchi, F. Croce, B. Scrosati, Electrochim. Acta 40 (1990) 991–997.
[29] K.G. Nair, A. Dufresne, Biomacromolecules 4 (2003) 1835–1842.
[30] K.G. Nair, A. Dufresne, Biomacromolecules 4 (2003) 657–665.
[31] K.G. Nair, A. Dufresne, Biomacromolecules 4 (2003) 666–674.
[32] G.B. Appetecchi, J. Hassoun, B. Scrosati, F. Croce, F. Cassel, M. Salomon, J. Power Sources 124 (2003) 246–253.